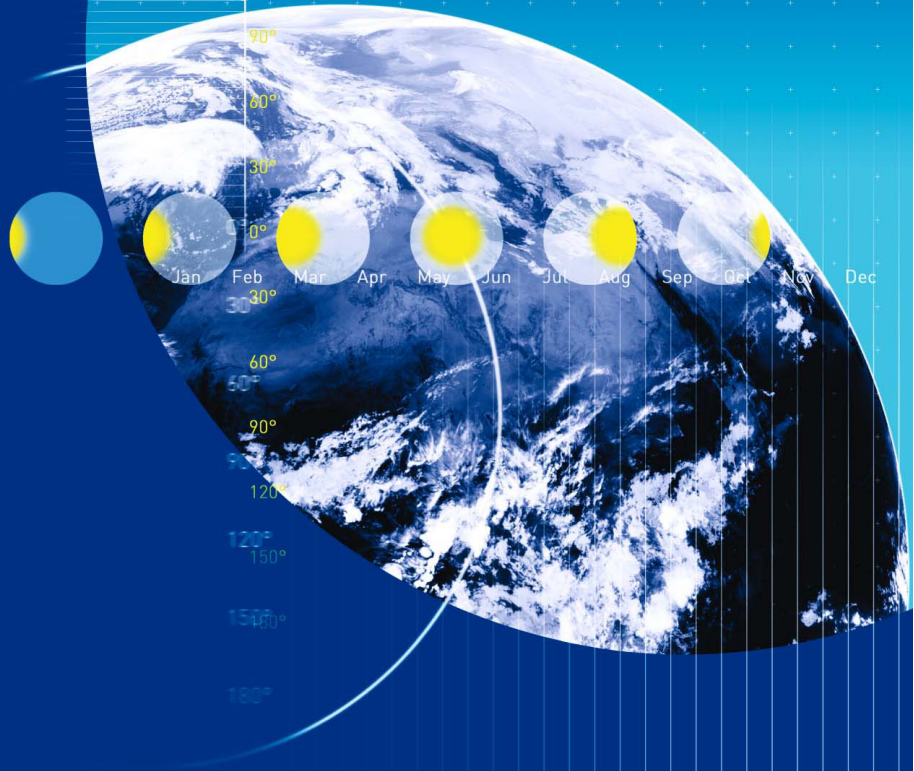


Handbook Part III: Theory Part 2

METEONORM

Global Meteorological Database
for Engineers, Planners and Education
Version 5.0 – Edition 2003
Software and Data on CD-ROM



A tool for Solar Energy Applications
Building Design, Heating & Cooling
Renewable Energy System Design
Agriculture and Forestry, Environmental Research
Meteorological Reference



The Swiss Federal Office of Energy supports
the development of METEONORM.

7 Theory Part 2: Temperature and Additional Parameters

7.1 Temperature generation

7.1.1 Introduction

Any temperature values provided must conjoin with the global radiation time series, as daily temperature variations and solar radiation are inter-linked. For example, temperature is an important factor for simulation of solar energy systems (PV or thermal). The combination of solar radiation and temperature is critical in assessment of heating and cooling loads in buildings. The production of stochastically generated radiation data sets in isolation is not enough to help in such applications.

From the interpolation and radiation generation procedure described above, hourly values of global radiation and monthly temperature required for temperature generation are now available at all points. Using these, hourly temperature values may be calculated as follows.

In *METEONORM* Versions 2–4 a model based on Scartezzini (1992) was used. In version 5.0 a completely new model is introduced. This model was developed in the framework of the EU IST project SoDa.

The idea underlying the model is still based on the assumption that the amplitude of the temperature variation during daytime is approximately proportional to the amplitude of the daily global radiation profile. Thus the temperature profile is calculated by transforming the radiation profile.

The model consists mainly of three parts:

1. The stochastic generation of daily values, based on monthly temperature and daily radiation values and measured temperature distributions.
2. The calculation of daily minimum and maximum temperatures, based on daily temperature values and daily and monthly radiation values.
3. The generation of hourly values, based on daily minimum and maximum temperature values and hourly radiation values.

7.1.2 Estimation of daily mean air temperatures

The daily temperature prediction problem faced was addressed by creating a new worldwide database describing the statistical patterns of observed temperature data across the world in different months of the year. The detailed description of this temperature database and its development is provided in Chapter 7.1.2.3. It is described how this statistical temperature data resource accessible to the generation process was created for approximately 8'000 stations using the Globalsod data prepared by the US National Climatic Data Centre (NCDC) covering the period 1994–2001.

A new and very fast generation process has been developed which draws on this database. It is described in Chapter 7.1.2.1.

7.1.2.1 Stochastic generation

First, an auto-regressive AR(1) process is run with almost no boundary settings. Then the distribution is mapped to the measured or interpolated distribution (according to the input), drawing on the statistical temperature data base resource.

Auto-regressive process

The auto-regressive process for daily temperature is executed in the following way:

$$\begin{aligned}
 Ta_d(dy) &= Ta_d(dy-1) + \delta T \\
 \delta T &= dT' + r \cdot dT'_{sd} \\
 r &= N(0,1) \\
 dT' &= \frac{dT(dy-1) + dT(dy)}{2} \\
 dT'_{sd} &= \frac{dT_{sd}(dy-1) + dT_{sd}(dy)}{2}
 \end{aligned}
 \tag{7.1.1}$$

where, dT is the mean day to day difference, dT_{sd} is the standard deviation of the day to day difference, dy is the day number in the month and r is a normally distributed random variable with expected value 0 and standard deviation 1.

The temperature database is accessed to gain temperature data at the selected site using the nearest site interpolation procedure. This provides the statistical data needed to estimate dT' and dT'_{sd} which are needed to carry out the auto-regressive operation described by Equation 7.1.1. The stochastically generated time series of hourly global solar radiation is of course produced first as it is the temperature driving agent in this procedure. Both difference values are varied according to the calculated daily insolation. If this is above 50% of the clear sky value, the measured "mostly clear sky" value is used, otherwise the "mostly overcast" value is used. In order to get a more realistic daily difference, the mean of the current and the previous day is taken for both values.

This process is first run without any limitations on the minimum, maximum or mean values. After the generation of each month, a check is made whether the difference between the month's last daily value and the mean of the current and the following month is more than 4°C. If so, a correction term is introduced in order to keep the above difference below 4°C. The monthly mean of December is taken as the first value.

Mapping the distribution

After the generation and the application of the end of month correction, the daily values are mapped to the measured mean distribution, which is interpolated between the 7 stored quantiles (see "Input variables extracted ..." below). This produces mean distributions and not extreme distributions. This means a statistically normal year is generated. Additionally, the yearly one day minimum is adopted as the January minimum in the northern hemisphere, or as the July minimum in the southern hemisphere and the yearly one day maximum is adopted as the summer (July/January) maximum in order to include mean one year extremes and not only monthly extremes.

The 4 days minimum temperature is calculated for January (in the northern hemisphere) or for July (in the southern hemisphere). This value is introduced in order to reproduce minimum design temperatures, which are normally defined using a period of several days.

If the generated 4-day minimum is more than 0.25°C higher than the measured value, the 4 days with the lowest minimum temperature are corrected to the measured value. If the difference is below 1°C, no changes to other days are made. If it is above 1°C the following 4 days or the 4 days before (dependent on the day of month) are raised in order not to change the monthly mean.

Input database

The Globalsod dataset was used. It contains approximately 8'000 stations worldwide with daily values and is accessible by internet. The data was collected by the National Climatic Data Center (NCDC), USA from national weather services.

Gathering data from each national meteorological service separately would have been both impractical and unaffordable to the SoDa and METEONORM project and could not have been finished in the short time needed.

As for quality control, the data did undergo extensive automated control (by USAF, over 400 algorithms) to correctly 'decode' as much of the synoptic data as possible, and to eliminate many of the random errors found in the original data. Then, these data were controlled further as the summary daily data were derived. However, a very small percentage of errors still remain in the summaries of daily data.

The data of the 8 years 1994–2001 are used. Table 7.1.1 shows the number of stations in different continents. The worldwide total is 5'805 stations (not all of the 8'000 stations could be used), all with monthly data available. One drawback is that a 8 year period is climatologically rather short. But at least the data give a hint about the recent temperature distribution of a location and include any warming in the last decade of the century. The recent warming, widely interpreted as due to man induced climate change, will most probably continue.

Tab. 7.1.1: Distribution of stations with temperature of the Globalsod database.

Region	Number
Europe without Russia	1'408
Asia with Russia	1'672
Africa	300
North America	1'401
South America	362
Australia and New Zealand	662
World	5'805

The data of the nearest stations is used to get interpolated values. The station network is not very dense in Africa, but fortunately, yearly temperature variations are smaller near the equator and therefore the spatial variations are not big compared with higher latitudes.

Input variables extracted for the assessment of temperature distributions

The monthly mean temperature and the hourly radiation values (all days and clear sky) are needed as inputs.

The following temperature parameters are used as statistical values:

- Monthly distribution of the daily temperature. Here 7 points of the monthly distribution are stored (1/31, 3/31, 6/31, 15/31, 25/31, 28/31, 30/31 quantiles).
- Monthly mean temperature
- Monthly mean of daily minimum and maximum hourly temperatures
- Mean monthly minimum and maximum hourly temperatures
- Mean standard deviation and difference of day to day variation, separated for days below and above the average daily difference between maximum and minimum temperatures. This approximately corresponds to a separation into clear and overcast days or days with high and low radiation.

Additional yearly values needed in order to reproduce yearly extremes:

- Mean minimum daily temperature per year
- Mean 4 day minimum temperature per year
- Mean maximum daily temperature per year

These values have to be estimated from the measurements at the available sites. The extreme values are estimated in the winter and summer period of each station. This procedure also works for interpolated monthly means. Here the statistical values of the nearest stations were used. The statistical values are adjusted by the difference of mean monthly temperatures between the actual site and temperature reference sites.

7.1.2.2 Daily minimum and maximum temperatures

The daily minimum and maximum temperatures are also calculated with help of the input data.

First, the monthly factor dX is calculated with measured monthly input values:

$$dX = \frac{\overline{Ta_{d,max}} - \overline{Ta_{d,min}}}{Gh_m} \quad (7.1.2)$$

with $\overline{Ta_{d,max}}$ and $\overline{Ta_{d,min}}$ as the monthly mean daily minimum and maximum hourly temperatures and G_m the monthly mean global radiation. This gives the general factor for conversion from radiation to temperature.

Then the daily difference between the maximum and minimum temperature is calculated using the daily radiation value Gh_d :

$$\Delta Ta_d = Gh_d \cdot dX \quad (7.1.3)$$

The daily minimum and maximum temperatures are calculated using this daily difference, a step based on the assumption that the mean value is the mean of the extreme daily values.

$$\begin{aligned} Ta_{d,min} &= Ta_d - \Delta Ta_d / 2 \\ Ta_{d,max} &= Ta_d + \Delta Ta_d / 2 \end{aligned} \quad (7.1.4)$$

A check is made to ensure that the daily extremes are within the limits set by the monthly extreme hourly values. If the monthly extremes are not equal (a difference of 0.5°C is allowed), the calculated maximum and minimum values are set to the monthly extremes.

7.1.2.3 Deriving the temperature profile from the irradiance profile

This model was derived in SoDa by M. Dumortier (2002).

First, a term showing the response of the air temperature to the solar radiation input is introduced. This ratio is called the ground to extraterrestrial irradiation ratio: kx . This is the ratio of the amount of solar radiation received on the ground since sunrise, to the amount of solar radiation that a surface perpendicular to the sunrays would have received during the same period:

$$kx(t) = \frac{\int_{sunrise}^t Gh(t) dt}{\int_{sunrise}^t G_0 dt} \quad (7.1.5)$$

Gh is the global horizontal irradiance

G_0 is the solar constant: 1367 W/m^2

It was shown that the variations of the temperature follow the variations of kx . The temperature increases when kx increases. The temperature reaches its maximum value at the same time as kx reaches its maximum (kx_{max}). When kx decreases, the temperature decreases.

It was concluded that during daylight hours the temperature varies linearly with the kx coefficient. The slope of this linear relationship seems to depend on the sky conditions. It also seems to be different before the maximum value of kx has been reached and afterwards. Finally, it is certainly influenced by incoming air masses.

These conclusions lead to the following Equation (7.1.6) for the slope:

$$slp_{before\ kx_{max}} = \frac{Ta_{d,max} - Ta_{d,min}}{kx_{max}} \quad (7.1.6)$$

$$slp_{after\ kx_{max}} = 1.7 \cdot slp_{before_{max}}$$

This slope is used to calculate the hourly temperature values during daytime:

$$t_{sunrise} < t \leq t_{kx_{max}} : \\ Ta(t) = Ta(t_{min}) + slp_{before_{max}} \cdot kx(t) \quad (7.1.7)$$

$$t_{kx_{max}} < t \leq t_{sunset} : \\ Ta(t) = Ta(t_{max}) - slp_{after_{max}} \cdot (kx_{max} - kx(t))$$

During night the temperature variation is mainly influenced by the amount of clouds.

To characterize the sky conditions, we used the Perraudau nebulosity index: IN (Perraudau, 1986). IN is based on the diffuse fraction and normalizes the value by taking the clear sky as a reference (Eqn. 7.3.1).

In order to define the night time nebulosity, the values between the last value of the day and the first value of the following day are interpolated linearly. As last and first value a limit of solar elevation of 5° was set.

The night time cooling rate (NCR) was set to:

$$NCR = 0.231 + 0.458 \cdot IN \quad [^\circ\text{C}/\text{hour}] \quad (7.1.8)$$

This cooling rate is only used for the first day of the generation, because the daily minimum and maximum values define the cooling rates:

For day 1, before sunrise :

$$Ta(t) = Ta(1) - NCR(1) \cdot t$$

For day 1, after sunset and any other day :

(7.1.9)

$$NCR(j) = \frac{Ta_{sunset}(j) - Ta_{d,min}(j+1)}{t_{sunset}(j) - t_{sunrise}(j+1)}$$

$$Ta(t) = Ta(t_{sunset}) - NCR(j) \cdot (t - t_{sunset})$$

These algorithms are defined for middle latitudes. For polar regions, special cases have to be defined (e.g. a virtual maximum daylength of 19 hours).

7.1.3 Validation

The totally new model for version 5.0 was tested at 6 stations in the USA and Switzerland (Tab. 3.3.3). In general, validation of the model produced satisfactory results. Although the model was changed, the test produced very similar results as with the model used in version 4. Generated daily temperature profiles are, however, somewhat too flat and lie too near the monthly average. The minima and maxima in winter are well reproduced, the summer maxima are somewhat lower than the observed maxima. The average values are automatically corrected. The generator produces good distributions (Fig. 7.1.4). The mean extreme values are calculated well now (Fig. 7.1.5).

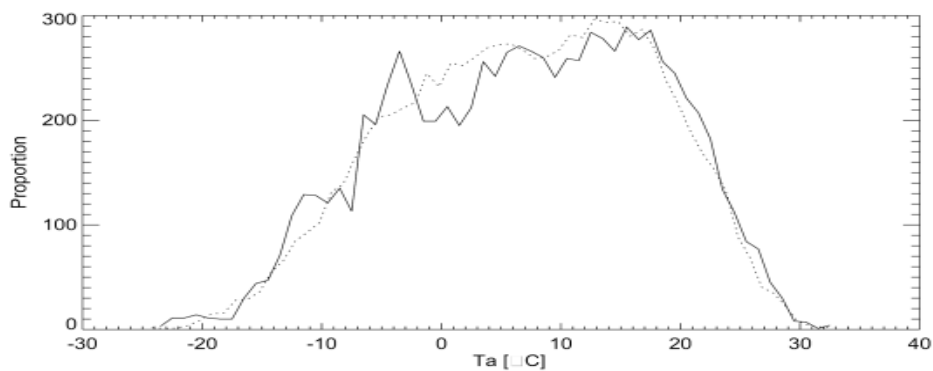


Fig. 7.1.4: Distribution of hourly values of 3 generated (broken line) and 10 measured years (1981–90) (line). Temperature for **Portland MN, USA**.

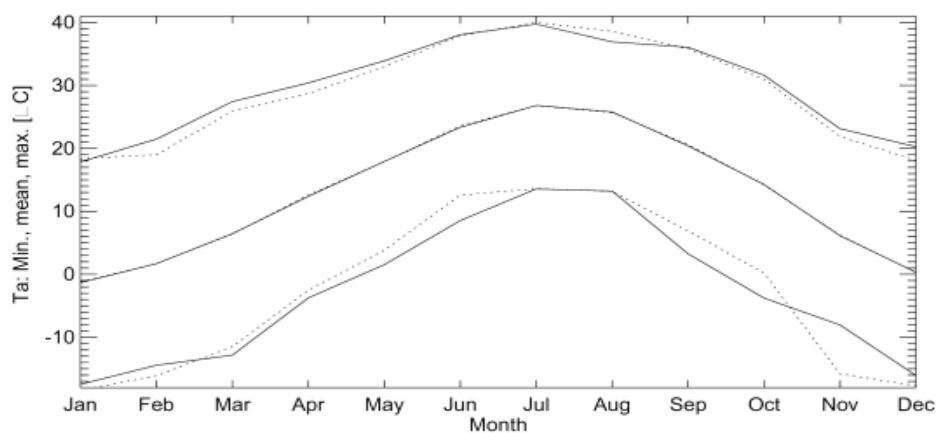


Fig. 7.1.5: Minimum and maximum hourly temperature values per month for **Dodge City, KS, USA**. Comparison between 3 generation runs (full lines) and the measured data for the years 1981–90 (broken lines). Average minimum and maximum (<Ta max>) and absolute maximum (Ta max).

Owing to the fact that the radiation generator produces symmetrical values with respect to solar altitude, the temperature generator also produces symmetrical daily profiles. Particularly for high solar altitudes, this leads to discrepancies between the calculated and measured standard daily profiles. Nevertheless, for most regions the mean temperatures per hour are calculated well (Fig. 7.1.6). The standard deviation of the midnight temperature differences (Figs. 7.1.7 and 7.1.8) is well reproduced. The distribution of the daily values and their variation are well reproduced despite the fact that these are not generated in an intermediate step. Figures 7.1.9 and 7.1.10 show examples of daily values of temperature for a continental (Fairbanks) and a oceanic (Seattle) site.

Figure 7.1.11 show the hourly variations for 2 typical days. The hourly temperature values are based on the radiation profile, but do not follow each variation of the radiation curve. The maximum temperature at the partly sunny day is reached 2 hours earlier than at the sunny day.

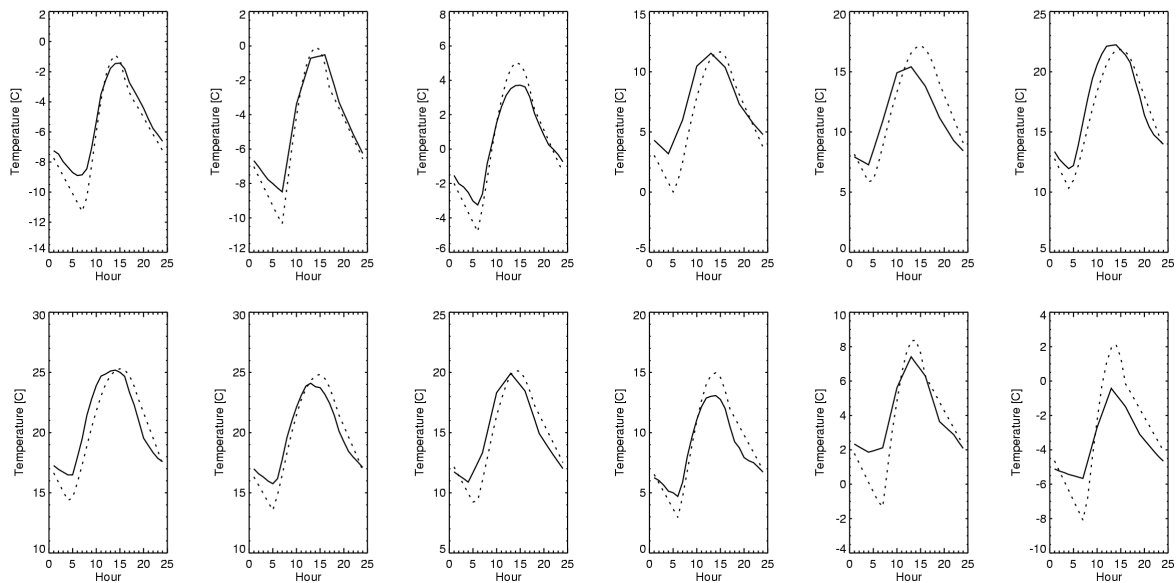


Fig. 7.1.6: Comparison of measured and generated mean temperatures per hour and month in **Portland** (ME, USA) (January–December). Full lines: measured (1981–90), broken lines: generated.

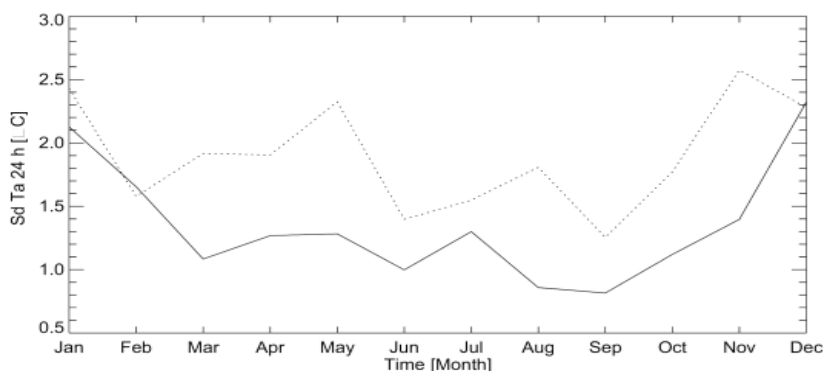


Fig. 7.1.7: Monthly standard deviations of midnight temperature differences for **Seattle** (WA, USA). Full lines: 3 generated runs, broken lines: measured (1981–90).

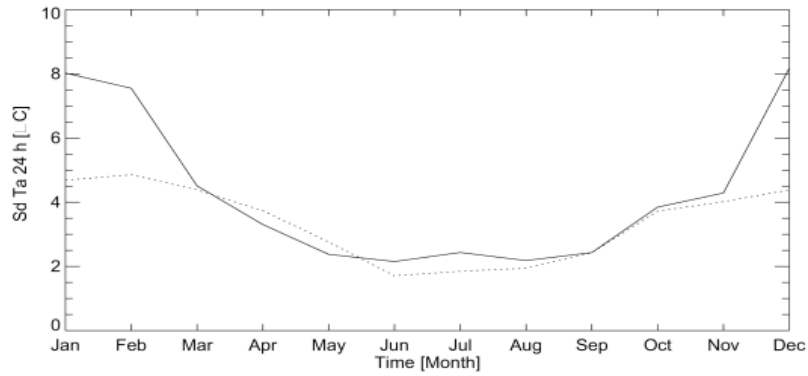


Fig. 7.1.8: Monthly standard deviations of midnight temperature differences for **Fairbanks** (AK, USA). Full lines: 3 generated runs, broken lines: measured (1995–98).

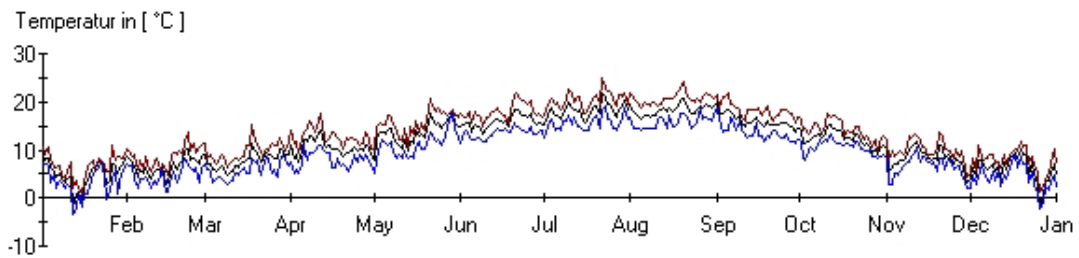


Fig. 7.1.9: Daily values of temperature (minimum, mean and maximum) generated for **Seattle** (WA, USA).

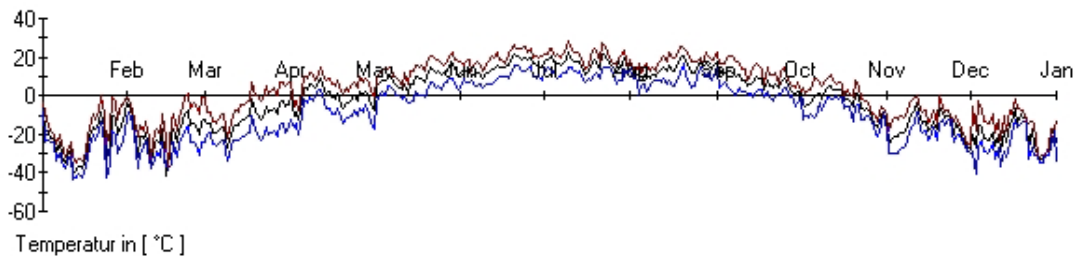


Fig. 7.1.10: Daily values of temperature (minimum, mean and maximum) generated for **Fairbanks** (AK, USA).

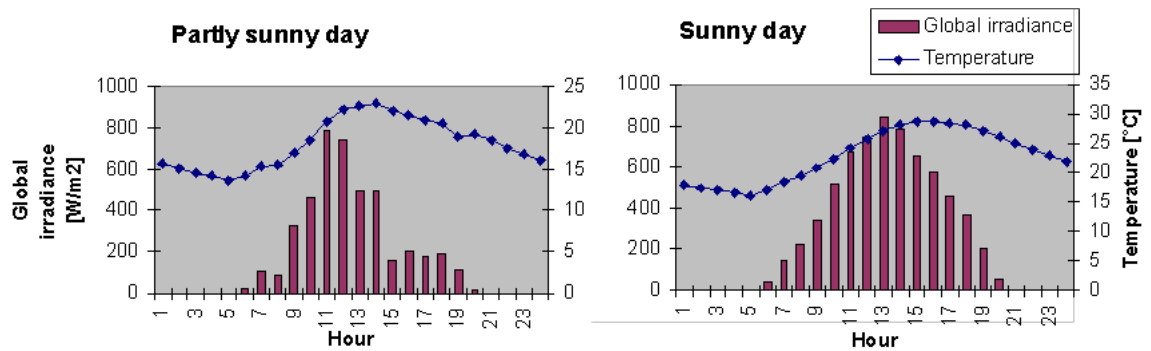


Fig. 7.1.11: Example of hourly values of temperature and global irradiance for 2 different types of days (partly sunny, sunny) for **Locarno-Magadino** CH.

7.2 Generation of supplementary parameters

METEONORM endeavours to provide suitable interfaces for most design programs in common use in photovoltaics, solar thermal applications and building simulation. For this, a range of output formats is provided. Several of these programs require further meteorological parameters in addition to global radiation and temperature. To provide these formats, simple formulae are presented below for estimating the required parameters. The additional parameters are referred to as supplementary parameters to distinguish them from the main parameters, i.e. radiation and temperature, described in the previous chapters. For a number of supplementary parameters, monthly values can only be obtained by first calculating hourly values. For certain parameters, calculation of hourly average values is not necessary if a meteorological or DRY station is chosen.

The principal problem in simulating further parameters is to ensure their compatibility with the previously obtained parameters. The approximate formulae and methods are described below. The supplementary parameters are not of the same quality as the main parameters (global radiation and temperature) and were not validated in an equally comprehensive way. Most adaptations were made using data from 15 weather stations in the USA and Switzerland (Tab 3.2.2).

The following supplementary parameters are calculated in *METEONORM*: Dew point temperature, relative humidity, mixing ratio, wet-bulb temperature, cloud cover, global and diffuse brightness, longwave radiation (incoming, vertical plane, outgoing), wind speed, wind direction, precipitation, driving rain, atmospheric pressure and UV radiation (UVA, UVB, erythemal, global and diffuse). The computational algorithms for the supplementary parameters are described below.

7.2.1 Dewpoint temperature and relative humidity

Dew point temperature (T_d) and relative humidity (RH) are related. Using Eqn. 7.2.1, the dew point temperature can be calculated from the relative humidity (Iribarne and Godson, 1981) and the relative humidity from the dew point temperature using Eqn. 7.2.2 (DWD, 1979).

$$T_d = \left[\frac{1}{T_a + 273.15} - (1.85 \cdot 10^{-4}) \cdot \log \left(\frac{RH}{100} \right) \right]^{-1} - 273.15 \quad (7.2.1)$$

Ta: Air temperature [°C]

Td: Dew point temperature [°C]

RH: Relative humidity [%]

$$RH = 100 \cdot \left(\frac{e_s}{e} \right)$$

$$e(T_a) = 6.11 \cdot \exp \left(\frac{17.1 \cdot T_a}{234.2 + T_a} \right) \quad (7.2.2)$$

$$e_s(T_d) = 6.11 \cdot \exp \left(\frac{17.1 \cdot T_d}{234.2 + T_d} \right)$$

e: Saturated vapor pressure at Ta [hPa] e_s : Saturated vapor pressure at Td [hPa]

While endeavouring to find a simple definition, it was discovered that the relative humidity at sunrise hours is a linear function of average humidity (Eqn. 7.2.3).

$$RH_{m,06}(m) = 23 + 0.79 \cdot RH(m) \quad , \quad 30 < RH_{06}(m) < 95 \quad (7.2.3)$$

This Equation was adjusted for 30 stations in the USA ($r^2 = 0.80$). The humidity at sunrise is further adopted to the daily clearness index:

$$RH_{d,06}(m) = RH_{m,06}(m) - 30 \cdot (Kt_d - Kt_m) \quad , \quad 25 < RH_{06}(m) < 97 \quad (7.2.4)$$

The dewpoint temperature at sunrise hours (here written as 6.00) is then calculated using Eqn. 7.2.1. The dewpoint temperature for each hour is calculated by linear interpolation between the sunrise values. Additionally (as a new feature in version 5) two different sinus functions were added depending on the amount of monthly radiation. If radiation is higher than 100 W/m^2 (a threshold for low radiation means) the following function is used:

$$Td_{\text{variations}}(h) = 0.5 + 0.5 \cdot \sin\left((h+1) \cdot \frac{\pi}{6} - \frac{3\pi}{4}\right) \quad (7.2.5)$$

This function has two maximum values at 08.00 and 20.00 and two minima at 02.00 and 14.00. For days with less than 100 W/m^2 the Eqn. 7.2.6 is used, which has only one maximum at 15.00:

$$Td_{\text{variations}}(h) = 0.5 + 0.5 \cdot \sin\left((h+1) \cdot \frac{\pi}{12} - \frac{3\pi}{4}\right) \quad (7.2.6)$$

These Equations were adapted to different measurements in the USA and Switzerland and reflect typical profiles.

The relative humidity for each hour is calculated using Eqn. 7.2.2.

Following this, the monthly values of generated data are fitted to the measured monthly average values by increasing the generated hourly values by the difference between generated and measured monthly average values. The corrections were mainly added at lower values of humidity, in order to avoid too many values with 100 % relative humidity. The differences are usually small (in the region of a few percent).

7.2.1.1 Validation

A short validation based on visual comparisons has been made at 7 stations (Tab. 7.2.1):

Tab. 7.2.1: Model sites. Climate zones according Troll and Paffgen (1981).

Name	Lon [°]	Lat [°]	Alt [m]	Year	Climate zone
Salt Lake City USA	111°58'W	40°77'N	1288	TMY	III, 10
Miami FL USA	80°17'W	25°49'N	17	TMY	V, 1
Portland ME USA	70°19'W	43°39'N	19	TMY	III, 8
Bern-Liebefeld CH	7°25' E	46°56'N	565	2001	III, 3
Davos CH	9°51'E	46°49'N	1'590	2001	III, 3
Locarno-Magadino CH	8°53'E	46°10'N	197	2001	III, 3
Jerez de la Frontera E	6°10'W	36°40'N	50	2000–2001	IV, 2

The distributions and the mean daily profiles per month were compared (Fig. 7.2.1 to 7.2.4). The mean daily profiles (Fig. 7.2.5) as well as a plot of the mean hourly temperature vs. humidity (Fig. 7.2.6 and 7.2.7) were examined.

For both dry and wet climates the generated humidity values compare well with measured data. The differences between the climates can be distinguished clearly. Nevertheless we advise the user to check the outcomes of the humidity generation before using it for delicate simulation processes (like cooling).

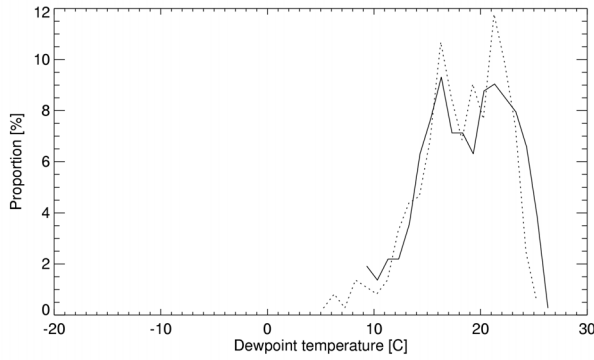


Fig. 7.2.1: Distribution of dewpoint temperature at **Miami FL USA**. Solid line = measured, broken line = generated values.

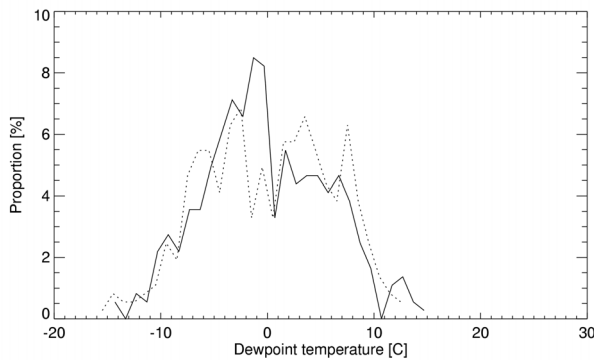


Fig. 7.2.2: Distribution of dewpoint temperature at **Salt Lake City UT USA**. Solid line = measured, broken line = generated values.

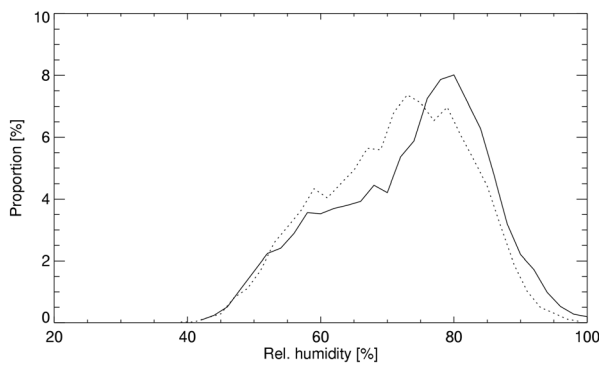


Fig. 7.2.3: Distribution of relative humidity at **Miami FL USA**. Solid line = measured, broken line = generated values.

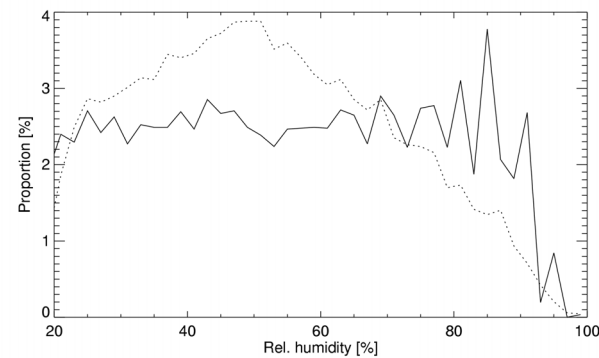


Fig. 7.2.4: Distribution of relative humidity at **Salt Lake City UT USA**. Solid line = measured, broken line = generated values.

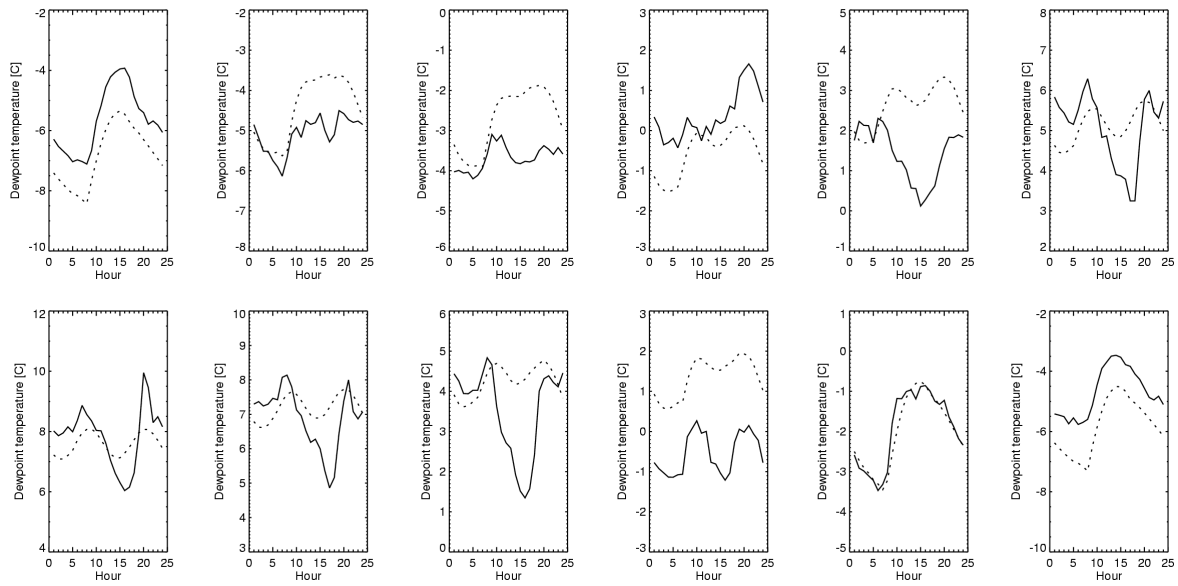


Fig. 7.2.5: Mean daily profile of dewpoint temperature at Salt Lake City UT USA. Solid line = measured, broken line = generated values. The second minimum after noon can be both seen at generated as well at measured values.

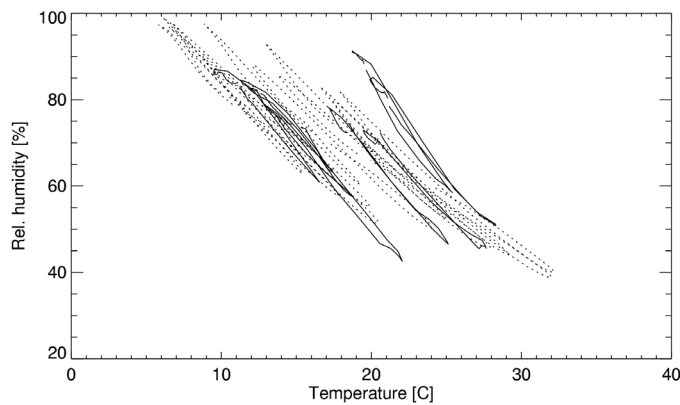


Fig. 7.2.6: Mean hourly humidity vs. temperature per month at Jerez de al Frontera E. Solid line = measured, broken line = generated values.

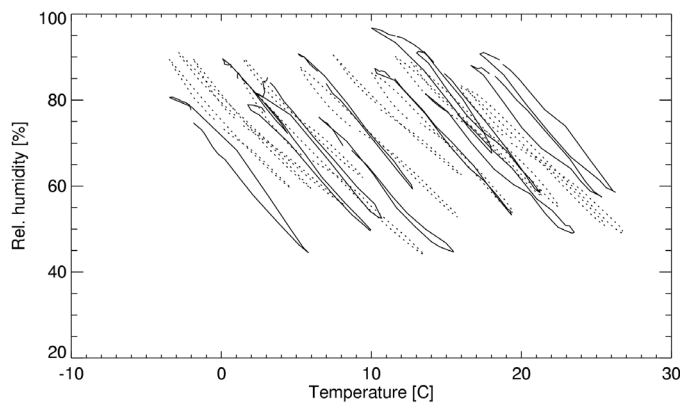


Fig. 7.2.7: Mean hourly humidity vs. temperature per month at Locarno-Magadino CH. Solid line = measured, broken line = generated values.

7.2.2 Wet-bulb temperature and mixing ratio

For the calculation of wet-bulb temperature, a new approximation is used (Stull, 1995):

Step 1: find height of lifting condensation level (LCL):

$$H_{LCL} = 0.125 \cdot (Ta - Td) \quad [\text{km}] \quad (7.2.7)$$

Step 2: calculate temperature of LCL (with dry lapse rate of 9.8°C/km):

$$Ta_{LCL} = Ta - 9.8 \cdot H_{LCL} \quad [^\circ\text{C}] \quad (7.2.8)$$

Step 3: moisture contents (**mixing ratio**: mass of water vapor to mass of dry air):

$$r_s = 0.622 \cdot \frac{e_s}{p - e_s} \quad [\text{g/g}]$$

$$r_d = 0.622 \cdot \frac{e}{p - e} \quad [\text{g/g}] \quad (7.2.9)$$

r_s : saturated mixing ratio [g/g] p : atmosphere pressure at station altitude [hPa]
 e_s : saturated vapor pressure [hPa] e : vapor pressure [hPa]
 r_d : mixing ratio [g/g]

4. step: saturated-adiabatic lapse rate:

$$\Gamma_s = g_{cp} \cdot \frac{1 + 8711 \cdot r_s / (Ta + 273.15)}{1 + Lv_{cp} \cdot 8711 \cdot r_s \cdot 0.622 / (Ta + 273.15)^2} \quad [\text{K/km}] \quad (7.2.10)$$

where,

$$g_{cp} = \frac{g}{C_p} = 1000 \cdot 9.81 / C_p \quad [\text{K/km}]$$

$$Lv_{cp} = 2.5 \cdot 10^6 / C_p \quad [\text{K}]$$

$$C_p = 1004.67 \cdot (1 + 0.84 \cdot r_d) \quad [\text{J/kgK}] \quad (7.2.11)$$

Lv_{cp} : specific latent heat of evaporation divided through C_p

5. step : wet bulb temperature :

$$Tp = Ta_{LCL} + \Gamma_s \cdot H_{LCL} \quad , \quad Ta > Tp > Td \quad (7.2.12)$$

The Figures below show two comparisons of generated and measured mixing ratio distributions at Miami FL USA (Fig. 7.2.8) and Locarno-Magadino CH (Fig. 7.2.9) (Tab. 7.2.1).

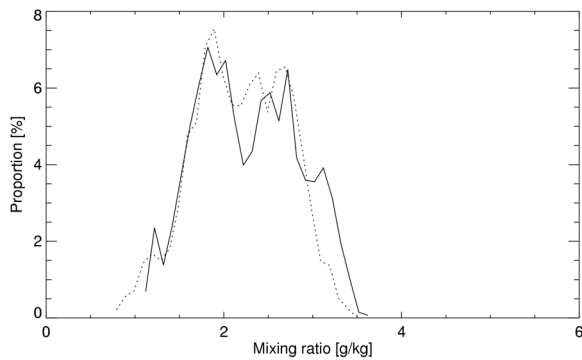


Fig. 7.2.8: Distribution of mixing ratio at **Miami FL USA**. Solid line = measured, points = generated values.

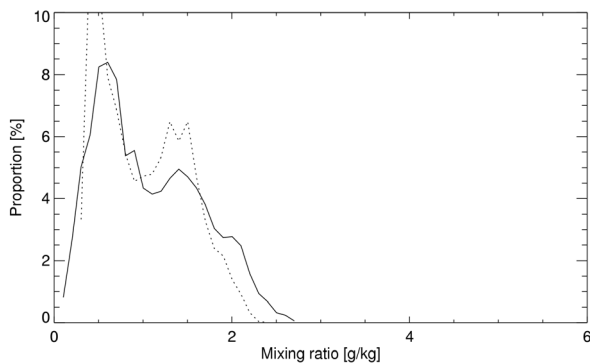


Fig. 7.2.9: Distribution of mixing ratio at **Locarno-Magadino CH**. Solid line = measured, points = generated values.

7.2.3 Cloud cover

Here too, a new model is used in version 5.0. The knowledge of the cloud cover index is essential for estimating the long wave radiation emitted by the atmosphere and for temperature modelling during night. The Equation of Kasten and Czeplak (1979) was used for calculating global radiation from clear sky radiation and the cloud cover index in two recent publications (Badescu, 1997; Gul et al., 1998). Initial checks with this model showed that it could be used for Europe and other temperate zones, but changes were needed for other regions. Additionally, when the Kasten and Czeplak algorithm was used in reverse to estimate cloud cover, it generally produced results biased towards cloud cover values that were too high.

Therefore, another model was investigated based on the Perraudau's nebulosity index. This index is also needed in the chain of algorithm for temperature generation and is defined as:

$$I_P = \frac{1 - D_h / G_h}{1 - D_c / G_c} \quad (7.2.13)$$

The cloud cover index relationship was looked into at Anchorage AK, Seattle WA, Salt Lake City UT, Raleigh NC and San Juan PR (Table 7.2.2) and a new formulation has been developed for all sites (Fig. 7.2.10):

If $0.07 < I_p < 1$

$$N = INT \left(8 \cdot \sqrt{\frac{1 - I_p}{0.825}} + 0.5 \right)$$

if $I_p \geq 1$

$$N = 0$$

if $I_p \leq 0.07$

$$N = 8$$

(7.2.11)

The denominator in the square route term in Equation 7.2.11, $a = 0.825$, is a mean value. Its value varies slightly with site location. Different models for specific sites have been constructed by varying the value of a . Because the differences were very small (Anchorage: $a = 0.802$, San Juan: $a = 0.794$), the use of one standard model is suggested.

Tab. 7.2.2: Model sites. Climate zones according Troll and Paffgen (1981).

Name	Lon [°]	Lat [°]	Alt [m]	Year	Climate zone
Anchorage USA	150.02 W	61.17 N	35	1990	II, 1
Seattle USA	122.30 W	47.45 N	122	1990	III, 2
Raleigh USA	78.78 W	35.87 N	134	1990	III, 8
Salt Lake City USA	111.96 W	40.77 N	1'288	1990	III, 10
San Juan PR	66.00 W	18.43 N	19	1990	V, 1

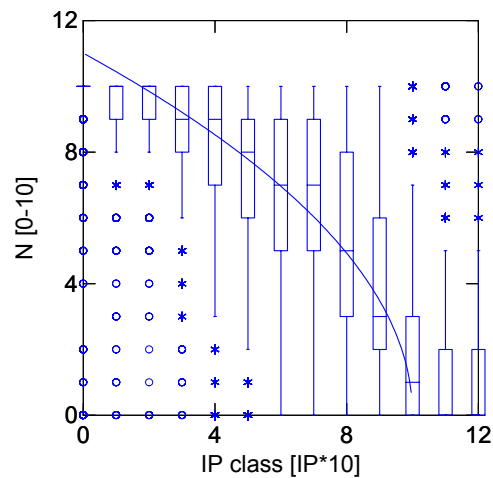


Fig. 7.2.10: Box plot of measured cloud cover (tenths) and model. Data of Anchorage, Seattle, Salt Lake City, Raleigh and San Juan 1990.

With stochastically generated data the distribution of Perraudau's index is significantly different. The generated IP values are lower than the measured ones. Therefore, this distribution has to be adapted to get accurate and bias free cloud cover information. A simple factor of 1.15 introduced to correct the generated I_{PC} :

If $0.06 < I_p < 0.869$

$$N = INT \left(8 \cdot \sqrt{\frac{1 - 1.15 \cdot I_{p,c}}{0.825}} + 0.5 \right)$$

if $I_p \geq 0.869$

$N = 0$

if $I_p \leq 0.06$

$N = 8$

(7.2.12)

The factor was found by iteration at the 5 test stations (Table 7.2.2).

The factor is calculated with the Index for elevation of the sun above 5° . For night hours the cloud cover is interpolated linearly between sunrise and sunset.

Validation with measured radiation data

The validation at the same stations gave the following results:

Tab. 7.2.3: Validation of cloud cover models:

Model	mbe	rmse
Perraudeau	-0.1	1.8
Kasten-Czeplak	0.4	2.2

The accuracy was significantly enhanced with the new model at the five sites. Additionally, the model is very simple and fast for computation and therefore very appropriate for use in *METEONORM*.

Validation with generated radiation data

The distribution and the mean values of all 5 sites together are better reproduced with the new method. The mean values are both 4.7 octas for generated and measured values. The histograms are given in Fig. 7.2.11. Generally, too many intermediate values are generated compared with the observed cloud cover.

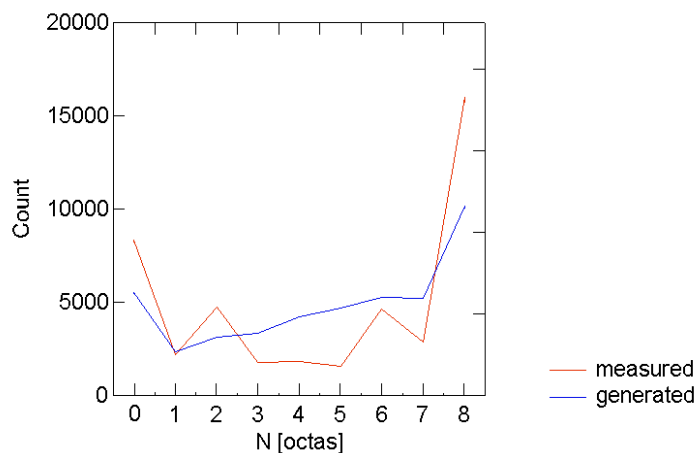


Fig. 7.2.11: Histogram of measured and generated cloud cover. Data of Anchorage, Seattle, Salt Lake City, Raleigh and San Juan 1990 and generated values with mean radiation values of 1961–90.

7.2.4 Longwave radiation

The longwave radiation (wavelength > 3 μm) is divided into two components:

1. Longwave horizontal radiation, **incoming** (L_{in}); radiation from the sky (upper hemisphere) on the horizontal plane (longwave incoming);
2. Longwave horizontal radiation, **upwards** (L_{up}); radiation from the earth's surface transmitted upwards (longwave outgoing).

The longwave radiation on a vertical surface (L_v) is derived from these two components. The radiation balance (R) may be determined from the two components (L_{in} and L_{up}) together with short wave radiation (global radiation) and albedo.

The new suggested model, as well as the above two existing models, have been validated using observed long wave data from 3 of the Baseline Surface Radiation Network (BSRN) stations, Payerne Switzerland, Boulder CO USA and Florianopolis Brazil. BSRN measurements are viewed as the world-leading source of high quality long wave radiation measurements.

7.2.4.1 Longwave radiation emitted from level ground

The outgoing longwave radiation from the ground is dependent on the temperature of the surface.

$$L_{\text{up}} = \varepsilon_g \cdot \sigma \cdot T_s^4$$

$$\sigma = 5.67 \cdot 10^{-8} \quad (7.2.13)$$

$$\varepsilon_g = 1.0$$

A preliminary investigation showed poor coincidence of existing models with BSRN data for hourly values. Therefore, a new model based on Swiss stations was developed. First a comparison between ground temperature estimated with Eqn. 7.2.13 and L_{up} at Payerne showed:

- that over grass the 5 cm temperature is the temperature of emission of the level ground and
- the emittance of natural ground ε_g is best set to 1.

Wind speed (measured at 10 m above ground) has been identified as an important factor. High wind speeds considerably lower the temperature differences between 2 m and 5 cm. If no wind speed data are available mean values of 3 m/s for the day and 1 m/s for the night can be used in sheltered regions.

During daylight hours, with G_h over 5 W/m^2 , the following formula has been established, yielding a r^2 value of 0.867 at all 5 Swiss SMI sites (hourly values).

$$T_s = T_a + [0.015 \cdot (1 - \rho) \cdot G_h - 0.7] \cdot \exp(-0.09 \cdot FF) \quad (7.2.14)$$

A new model for night time hours was introduced. This model was constructed using the data of Payerne. A maximum deviation of 4.7°C was found. Wind speed is even more important at night than during the day because of the higher stability of the planetary boundary layer. Very cold ground temperatures can only be reached when wind speed is very low.

$$T_s = T_a + [0.0006 \cdot N^3 - 0.037 \cdot N^2 + 0.376 \cdot N - 4.7] \cdot \exp(-0.218 \cdot FF) \quad (7.2.15)$$

For $T_{\text{am}} < -3^\circ\text{C}$, $\max(T_s) = 0^\circ\text{C}$ (correction for snow coverage).

7.2.4.2 Longwave radiation emitted by the atmosphere

The model of Aubinet (1994) is recommended after comparison with models of Dogniaux and Lemoine (1984), EMPA (1985) and Gabathuler and Marti (2000). Dogniaux and Lemoine used in ESRA, EMPA

models in *METEONORM*. Not only did the results speak for Aubinet, but the input parameters (T_d , G_h and G_c) are also easily available.

$$L_{in} = \sigma \cdot [94 + 12.6 \log(100 \cdot e_s) - 13 \cdot KT_c + 0.341 \cdot (Ta + 273.15)]^4 \quad (7.2.16)$$

In addition to the horizontal information incoming longwave radiation for vertical planes (facades) is provided. Here the formulation used in ESRA based on Cole (1979), which addresses the anisotropy, is used:

$$L_v = L_{in} \cdot 0.5 + 0.0031 \cdot [1 - N \cdot (0.7067 + 0.00822 \cdot Ta)] \cdot \sigma \cdot (Ta + 273.15)^4 + L_{up} \cdot 0.5 \quad (7.2.17)$$

7.2.4.3 Radiation balance

The radiation balance for horizontal surfaces can be calculated using shortwave and longwave parameters as well as albedo (ρ).

$$R = L_{up} - L_{in} + G_h \cdot (1 - \rho) \quad (7.2.18)$$

7.2.4.4 Conclusions on longwave radiation modelling

Although based on simple approximation of cloud cover and humidity, the long wave models show good results at the BSRN stations Payerne, Boulder and Florianopolis (Tab. 7.2.4).

The combination of the new models leads to a significantly higher accuracy for radiation balance than with any other tested combination.

Tab. 7.2.4: Error of estimation of hourly values of long wave radiation and ground surface temperatures. mbe means is the error, rmse root mean square error. The dewpoint temperature and wind speed used were generated stochastically.

Station (all BSRN)	R		Ldn		Lup		Ts	
	mbe	rmse	mbe	rmse	mbe	rmse	mbe	rmse
Payerne	0.3	20.8	-0.6	21.3	-0.6	10.4	-0.2	2.0
Boulder	2.3	48.0	18.3	29.1	4.4	13.1	-	-
Florianopolis	-	-	-4.3	23.5	-	-	-	-

7.2.5 Illuminance

Global and diffuse illuminance is calculated using generated global radiation with the Perez et al. (1990) model. A short comparison with TMY2 data at 7 stations throughout the USA (from Puerto Rico to Fairbanks) showed the following discrepancies (*METEONORM* – TMY2): Global illuminance: mbe: +0.17 klux, rmse: 0.55 klux; diffuse illuminance: mbe: +0.51 klux, rmse: 0.52 klux.

7.2.6 Wind

The provision of wind speed and wind direction in *METEONORM* is intended as an extension of its output for design programs requiring wind data as input. The wind itself is not usually of great importance for solar and building (energy) application, and the model presented here is not intended to provide more than a rough approximation of monthly average and distributions. The present interpolation should not be used for designing wind power plants. The problem of wind simulation for any desired location is practically insoluble, since wind speed is greatly influenced by local features, and spatial variations are very large. The average monthly value is very difficult to estimate without a detailed knowledge of local topography. Detailed information on wind conditions throughout Europe may be found in the European Wind Atlas (Risoe National Laboratory, 1990).

7.2.6.1 Wind speed

Despite the difficulties described above, hourly wind speed values were nevertheless generated. The model was adapted to 30 stations in the USA (Tab. 3.3.1) and 20 stations in Switzerland. It consists of a daily model based on average daily global radiation, and on an independent stochastic model:

$$FF'(h) = F_m(h, K_t) + F_t(h) \quad (7.2.19)$$

where $FF'(h)$ is the normal distribution of hourly wind speed, F_m is the daily model and F_t the stochastic model. The stochastic model is defined as a first order autoregressive process AR(1):

$$\begin{aligned} F_t(h) &= x_m \cdot F_t(h-1) + Z \\ Z &= m_w + s_w \cdot r(h) \\ m_w &= (1 - x_m) \cdot FFi(month) \\ s_w &= (1 - x_m^2)^{1/2} \cdot sdi(month) \end{aligned} \quad (7.2.20)$$

where $r(h)$ is a normally distributed random variable $N(0,1)$. x_m is calculated for the relevant climatic zone and continent:

Climatic zone 303 :

$$x_m = 1 - [-9.1 + 7.1 \cdot FFi(month)]^{-1}, \quad 0.75 < x_m < 0.99, \quad (7.2.21)$$

elsewhere:

$$x_m = 1 - [10.285 \cdot FFi(month)]^{-1}, \quad 0.75 < x_m < 0.99$$

The daily model F_m is calculated under local and climatic conditions with daily K_t and G_h values. The following categories were adopted:

Tab. 7.2.5: Categories adopted in the daily model

No.	Climatic zone	Local terrain
1	Europe, III, 3 (e.g. central Europe)	open
2	III, 3 (Switzerland alone)	lake
3	Alpine zones II - IV	mountain valley
4	Alpine zones II - IV	summit
5	I, 1 - 4, II, 1 - 3, III, 1 - 2 (cold and very cold regions)	general
6	IV, 1 - 7, V, 1 - 5 (tropics, subtropics)	lake, sea
7	III, 4 - 12 (e.g. continental regions of the USA)	general

In the daily model, the average values of the daily distribution of wind speed on clear days ($K_t > 0.45$, $G_h > 100 \text{ W/m}^2$) are stored for each terrain (Tab. 7.2.6). If the radiation values lie below the limiting values, no daily model is included.

Tab. 7.2.6: Daily model of average daily distribution (F_m) for clear days in each category. The values are normalized to 0.

Hour/climatic zone	1	2	3	4	5	6	7
1	-0.4	-0.1	-0.8	0.5	-0.3	-1.1	-0.7
2	-0.5	-0.2	-0.8	0.3	-0.4	-1.2	-0.7
3	-0.5	-0.2	-0.9	0.2	-0.4	-1.4	-0.8
4	-0.6	-0.2	-0.9	0.2	-0.5	-1.5	-0.9
5	-0.6	-0.1	-0.9	0.1	-0.6	-1.5	-0.9
6	-0.6	-0.3	-1.0	0.1	-0.6	-1.5	-0.9

7	-0.6	-0.4	-0.9	0.0	-0.6	-1.5	-0.9
8	-0.5	-0.4	-0.9	-0.2	-0.5	-1.4	-0.7
9	-0.2	-0.3	-0.7	-0.3	-0.3	-1.0	-0.4
10	0.0	-0.1	-0.3	-0.5	-0.1	-0.4	0.1
11	0.3	0.1	0.1	-0.5	0.0	0.3	0.5
12	0.5	0.2	0.7	-0.5	0.2	0.9	0.8
13	0.6	0.2	1.1	-0.5	0.4	1.4	1.0
14	0.7	0.2	1.6	-0.5	0.5	1.8	1.1
15	0.8	0.3	1.8	-0.4	0.7	2.1	1.2
16	0.8	0.2	1.9	-0.4	0.8	2.2	1.2
17	0.7	0.1	1.6	-0.3	0.8	2.1	1.2
18	0.6	0.1	1.2	-0.1	0.8	1.8	1.0
19	0.3	0.1	0.6	0.1	0.6	1.3	0.6
20	0.0	0.3	0.0	0.4	0.3	0.7	0.2
21	-0.1	0.3	-0.4	0.6	0.0	0.2	-0.3
22	-0.2	0.2	-0.6	0.7	-0.1	-0.5	-0.5
23	-0.3	0.1	-0.7	0.6	-0.2	-0.8	-0.6
24	-0.3	0.1	-0.8	0.6	-0.3	-1.0	-0.6

The hourly values ($FF'(h)$) were calculated using Eqns. 7.2.19 to 7.2.21 and then transformed to correspond to the distribution of hourly values for the site. It is assumed that the form of the distribution (f) corresponds to a Weibull distribution (SFOE, 1990) (Eqn. 7.2.21). Following transformation, the final values of $FF(h)$ are obtained.

$$f(FF) = \frac{k}{A} \cdot \left(\frac{FF}{A}\right)^{k-1} \cdot \exp\left[-\left(\frac{FF}{A}\right)^k\right] \quad (7.2.21)$$

The parameters A and k required in the Weibull distribution, as well as the standard deviation sdi , are estimated from wind speed (Eqns. 7.2.22 to 7.2.29). To determine the parameters k , similar local and climatic categories are used as for the daily model. The models were changed for version 4. In the current version, the parameter A and sdi are calculated mathematically.

1. Open or Sea/Lake:

Climate zone III:

$$k = 1.48 + 0.35 \cdot \log(FFi(month) - 2.07) \quad (7.2.22)$$

Climate zone IV, 1, latitude > 35°N or latitude < 35°S:

$$k = 1.21 + 0.29 \cdot \log(FFi(month) - 1.59) \quad (7.2.23)$$

Climate zone IV, 2 – 7, latitude > 35°N or latitude < 35°S:

$$k = 1.48 + 0.35 \cdot \log(FFi(month) - 2.07) \quad (7.2.24)$$

Climate zone IV, V, 35°S < latitude < 35°N

$$k = 1.09 + 0.21 \cdot FFi(month) \quad (7.2.25)$$

2. Summits:

$$k = 1.37 + 0.243 \cdot \log(FFi(month) - 2.08) \quad (7.2.26)$$

3. Valleys, cities and sites with obstacles around:

$$k = 1.21 + 0.37 \cdot \log(FFi(month) - 1.22) \quad (7.2.27)$$

Calculation of A and sdi :

A and sdi are dependent on k :

$$A = FFi(month) \cdot \left[\left(\frac{1}{k} \right)! \right]^{-1} = FFi(month) \cdot \left[\Gamma \left(1 + \frac{1}{k} \right) \right]^{-1} \quad (7.2.28)$$

$$sdi = A \cdot \sqrt{\Gamma \left(1 + \frac{2}{k} \right) - \Gamma^2 \left(1 + \frac{1}{k} \right)} \quad (7.2.29)$$

Validation

The calculated hourly wind values were tested using data from 15 stations in the USA and Switzerland (Tab. 3.3.2). The validation was restricted to checking the distributions. The results showed good agreement between calculated and measured data (Fig. 7.2.12). The average monthly values of generated data come to the original (interpolated or station) values.

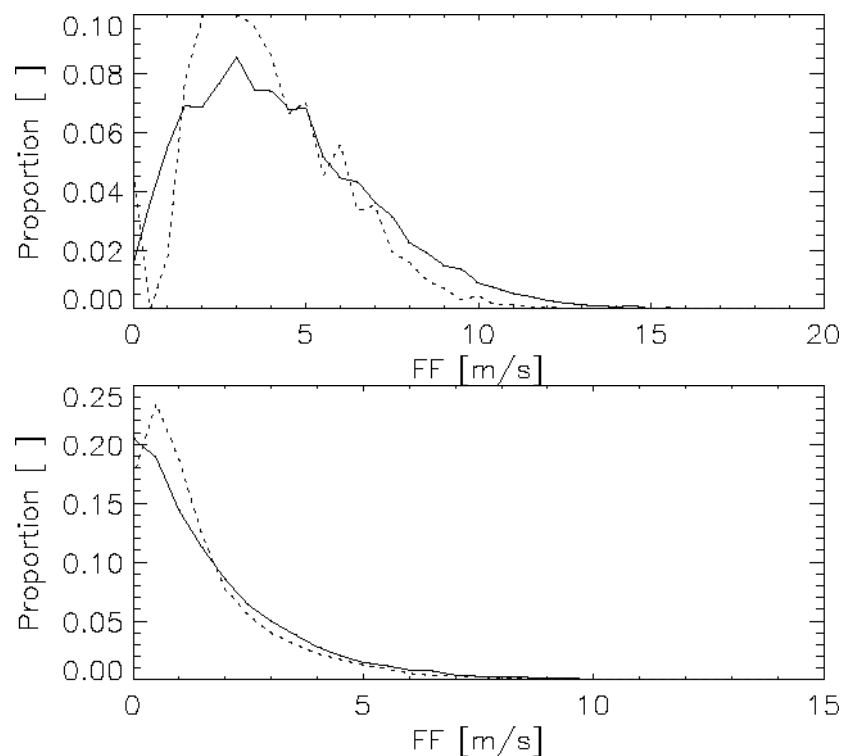


Fig. 7.2.12: Comparison between distributions of calculated (full line) and measured (broken lines) wind speed, showing data from Portland (MN, USA) (above), and Bern-Liebefeld (CH) (below).

7.2.6.2 Wind direction

A totally new wind direction generation process is used for version 5.

The basis of the model are approximately 100 stations with stored wind direction distributions (45°) for the months of January and July. Mainly data from ISMCS (NCDC, 1995) are used.

The nearest site is chosen as representative. The monthly distributions are calculated as a weighted average of the July and the January distributions. If monthly mean values of wind direction are available, the distribution are turned in order that the maximum value of the distributions matches the mean direction value.

The generation process is based on 3 steps:

1. Stochastic generation of an hourly time series of wind direction

$$DD'(t) = 0.914 + DD'(t-1) + N(0,1) \quad (7.2.30)$$

No relationship has been used between wind direction and other meteorological parameters.

2. Mapping of the generated values to the interpolated distribution (45° band with, 0 – 360°).

3. Overlying a second stochastic process in order to get finer resolution:

$$DD''(t) = 0.914 + DD''(t-1) + 8 \cdot N(0,1) \quad (7.2.31)$$

4. The definitive wind direction DD is calculated as sum of the two ARMA(0,1) processes:

$$DD(t) = DD''(t) + DD'(t) \quad (7.2.32)$$

The resulting wind roses look reasonable. Of course they can only be approximations. Two examples from the Atlantic Ocean are shown below (Sable Island / NS Canada and Izana Mountain Top / Canarias E). Both the west and the trade wind system are reproduced (Fig. 7.2.13 – 14).

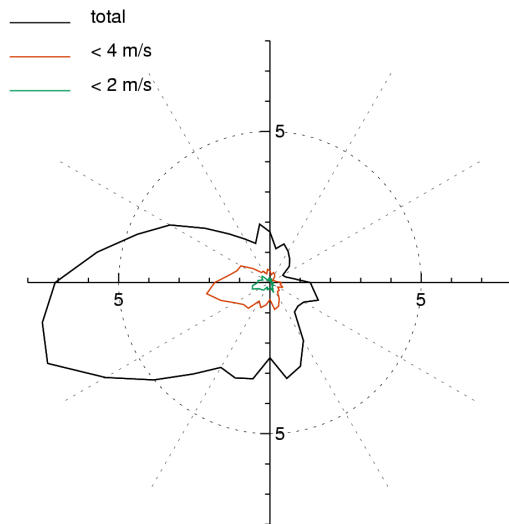


Fig. 7.2.13: Wind rose of Sable Island (west wind system).

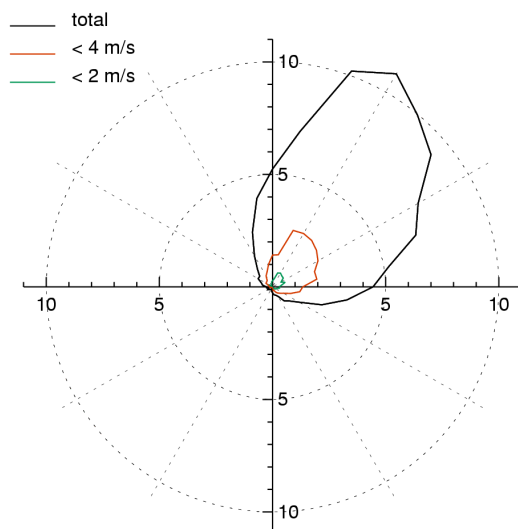


Fig. 7.2.14: Wind rose of Izana Mountain Top (trade wind system).

7.2.7 Atmospheric pressure

The atmospheric pressure at a particular station is set to the same value the whole year round. The model used for average air pressure assumes a polytropic atmosphere with constant temperature decrement (-6.5 °C/km) and constant temperature at sea level (15 °C) (7.2.33).

$$p = 1013 \cdot \left[1 - \frac{0.0065 \cdot z}{288.15} \right]^{5.264} \quad (7.2.33)$$

p: Atmosphere pressure [hPa] z: Height above sea level [m]

7.2.8 Heating degree days

The heating degree days (HDD) represent a simple and commonly used method for calculating the energy consumption of heated buildings. In Version 5.0 (as in the previous version), heating degree days are estimated using generated hourly temperature series. They can be calculated with the output formats LESOSAI or sia 380/1. The generated values have an accuracy of about 1% compared to the listed values in Switzerland (sia 381/2).

7.2.9 Precipitation

In former versions of *METEONORM*, precipitation was only available as monthly sums. A new generation process is introduced for version 5. It is based on the broad knowledge available from many publications of weather generation, which are mostly related with the WGEN generator (Richardson and Wright, 1984).

The reason for choosing new algorithm was that time series of precipitation are also needed in building simulation and that no existing method was based on solar radiation, which is available in this case. Generally the generation of the dry or wet days' time series is the first step. Additionally the existing generators are fitted to agricultural simulations, mostly provide only daily time series and are site dependent. The proposed method produces first daily precipitation series and then hourly values for every site worldwide.

7.2.9.1 Daily precipitation values

At the beginning of the generation process the worldwide, monthly values of precipitation and the number of days with precipitation above 1 mm are known. Additionally clear and all sky radiation, cloud amounts and temperature (ambient, dewpoint) time series are available. The produced time series correspond to mean monthly means.

Before the generation starts the number of days with precipitation above 0.1 mm (Rd_0) is calculated with the following Equation:

$$Rd_0 = INT \left[0.971 + 3.445 \cdot \frac{Rd_1}{RR_m} \right], \quad 0 < Rd_0 < Rd_1 \quad (7.2.34)$$

The Equation has been adapted to data of 25 European stations with measurements from 1901–99 ($r^2 = 0.726$).

A second value for the generation process is calculated: the mean amount of dry spells per month:

$$Ds = INT \left[22.041 - 6.507 \cdot \ln(Rd_1) \right], \quad 0 < Ds < ndays - Rd_0 \quad (7.2.35)$$

The Equation has been adapted to data of the same 25 European stations ($r^2 = 0.773$).

The generation process starts with finding the $n = Rd_0$ days with the lowest clearness indexes of the month. These days are assumed as days with precipitation. The days are sorted according to the clearness indexes. The lower the clearness index, the higher the precipitation is set.

The amount of precipitation per day is calculated with a Weibull distribution (Selker and Haith, 1990) also used in the ClimGen generator (<http://www.bsyse.wsu.edu/climgen/>).

$$RR_d(P) = 0.84 \cdot \frac{RR_m}{Rd_0} (-\ln(1 - P_n))^{1.333} \quad (7.2.36)$$

where $k = 1/1.333$ and $A = 0.84 * RR_m/Rd_0 = 1/\Gamma(1+1/k) * RR_m/Rd_0$ and

$$P_n = \frac{Rd_0 - n - 0.75}{Rd_0 - 0.5}, \quad 0 \leq n \leq Rd_0 - 1 \quad (7.2.37)$$

The cumulated probabilities P_n are stretched slightly. First tests have shown that the distribution are better reproduced this way.

The precipitation amount is summed for each month. If the sum differs from the interpolated mean the daily values are corrected by a factor.

If the generated dry spells are lower than the modelled ones (Eqn 7.2.35), the rainy days are moved by one day if possible in order to achieve the correct days with dry spells.

7.2.9.2 Hourly values

First the number of hours with precipitation (for days with precipitation) is calculated with the following Equation:

$$n_{rh} = INT \left[1.5 \cdot \left(\frac{4.096 \cdot RR_d}{RR_m} + 0.365 \cdot \frac{RR_m}{Rd_0} - 0.029 \cdot RR_d \right) \right] \quad (7.2.38)$$

The number of hours of precipitation is mainly dependent on the amount of precipitation per day (RR_d) and the mean intensity of the precipitation per day of the month (RR_m/Rd_0). The Equation was adapted to hourly precipitation data of Bern-Liebefeld, Neuchatel, Davos, Luzern and Locarno-Magadino with data of 2000 and 2001 ($r^2=0.815$). The numbers of hours are set between 1 and 24. This set of stations includes regions both south and north of the Alps with different kinds of precipitation regimes (advective and convective). The factor 1.5 was introduced due to lowering of the precipitation hours by other parts of the chain of algorithms. Mainly the time series of cloud cover limits the hours of precipitation.

Hours with precipitation have to fulfil a second condition: the mean cloud cover has to be at least 6 octas. If less hours with 6 octas are available per day, the number of hours are set to this lower value.

In a second step, the possibility of precipitation per hour is simulated with an autoregressive process and a mean daily profile. This is done because the possibility of precipitation is generally higher in the evening and the night than in the morning hours.

$$P_m(h) = 1 + 0.15 \cdot \sin\left(\frac{\pi}{2} + (h+1) \cdot \frac{2\pi}{24}\right) \quad (7.2.39)$$

$$P_s(h) = 0.7 \cdot P_s(h-1) + 0.2 \cdot N(0,1) \quad (7.2.40)$$

$$P_{RR_h}(h) = P_m(h) + P_s(h) \quad (7.2.41)$$

The hours with precipitation is moved to hours with 7 or 8 octas of cloud cover by enhancing the possibility at hours with 8 octas by 0.5 and at hours with 7 octas by 0.25. The possibility of precipitation is used to sort the hours with precipitation. If e.g. the day has 5 hours with precipitation the hours with the 5 highest values of P_{RR_h} are chosen and sorted.

The amount of precipitation per hour is defined with a Weibull distribution:

$$RR_h = 0.647 \cdot \frac{RR_d}{n_{rh}} \cdot [-\log(1 - P_n)]^{1.7} \quad (7.2.42)$$

where $k = 1/1.7$ and $A = 0.647 \cdot RR_d/n_{rh} = 1/\Gamma(1+1/k) \cdot RR_d/n_{rh}$ and

$$P_n = \frac{n_{rh} - n - 0.25}{n_{rh} - 0.5}, \quad 0 \leq n \leq n_{rh} - 1 \quad (7.2.43)$$

The cumulated probabilities P_n are stretched slightly. First tests have shown that the distributions are better reproduced this way. n corresponds to the sorted number of hours with precipitation according to the possibility (P_{RR_h}).

The generated hourly values are corrected in order to match the daily sums.

7.2.9.3 Validation

A short validation at 6 stations in Europe was performed (Tab. 7.2.7).

Tab. 7.2.7: Test sites for precipitation model.

Site	Source	Latitude [°,']	Longitude [°,']	Altitude [m]	Period	Time resolution
Bern-Liebefeld	Meteoswiss	46.56	7.25	565	2000–2001*	Hour
Locarno-Magadino	Meteoswiss	46.10	8.53	197	2000–2001*	Hour
Davos	Meteoswiss	46.49	9.51	1590	2000–2001*	Hour
Vaexjoe/Kronoberg	KNMI	56.87	14.80	166	1901–99	Day
Frankfurt	KNMI	50.12	8.67	103	1901–99	Day
Marseille	KNMI	43.31	5.40	75	1901–99	Day

* Figures in Tab. 7.2.8 have been adapted to mean values 1961–90.

The following points were investigated: Days with precipitation over a certain amount, maximum daily and hourly sums (mean values per year), mean maximum duration of dry and wet spells per year and hours of precipitation (Tab. 7.2.8).

Tab. 7.2.8: Comparison between measured and generated time series of precipitation.

Site	Type	RR>0 mm [days]	RR>1.0 mm [days]	RR>12.5 mm [days]	Max. daily sum [mm]	Max. hour. sum [mm]	Dry spell [days]	Wet spell [days]	RR [mm]	Prec. Hour [h]
Bern	Measured	170	126	24	47.2	19.0	13	17	1029	1107
Bern	Generated	167	126	23	40.5	13.5	9	9	1025	1034
Locarno	Measured	138	105	47	113.0	36.8	33	10	1773	1149
Locarno	Generated	118	101	42	87.5	29.1	18	5	1772	1084
Davos	Measured	181	129	26	70.1	10.6	14	11	1084	1371
Davos	Generated	165	129	26	44.3	15.2	13	8	1081	1053
Vaexjoe	Measured	186	117	14	32.3	-	16	14	652	-
Vaexjoe	Generated	181	113	12	23.4	8	10	10	610	893
Frankfurt	Measured	172	110	14	35.3		17	12	650	
Frankfurt	Generated	155	106	14	30.4	10.4	18	6	685	845
Marseille	Measured	83	56	20	65.2		33	7	596	
Marseille	Generated	80	60	13	36.1	12.2	28	9	545	523
Mean difference	%	-7 %	-1 %	-10 %	-27.8 %	-12.8 %	-24 %	-33 %	-1 %	-25 %

Days with precipitation are reproduced well. Especially the lower thresholds ($RR_d > 0\text{mm}$, $RR_d > 1\text{mm}$) are given precisely. Monthly and yearly sums correspond to input values. Small differences in the table are induced by different time periods. The maximum daily sum is calculated too low (-28%). The maximum hourly sum is calculated quite precisely. The amount of wet and dry spells are calculated too low. This is mainly induced by the fact that the calculations are fitted to monthly means and not to yearly means. The number of hours with precipitation is also too low. Nevertheless, the deviations the different magnitudes of the precipitation for the different climates are clearly observable.

In the following figures two time series of hourly precipitation for Bern-Liebefeld are shown. Figure 7.2.15 shows a generated time series, 7.2.16 a measured time series (year 2000).

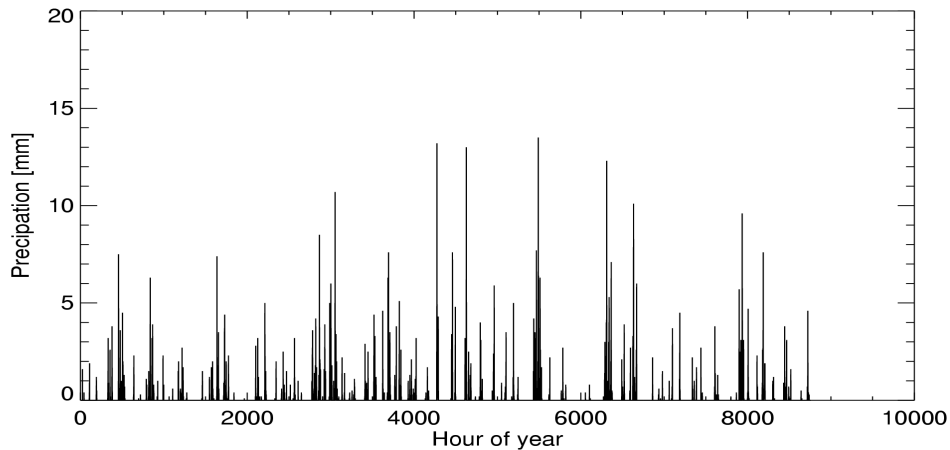


Fig. 7.2.15 Generated time series for Bern-Liebefeld.

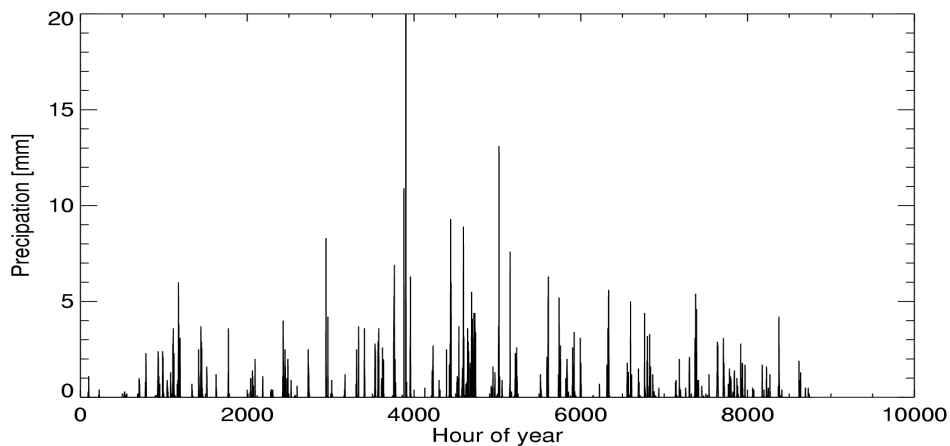


Fig. 7.2.16 Measured time series for Bern-Liebefeld (year 2000).

7.2.9.4 Driving rain

Driving rain is rain that is carried by the wind and driven onto the building envelope (façades and roofs). It is a complex phenomenon of falling raindrops in a turbulent flow of wind around a building. It is one of the important climatological factors which determine long-term use and durability of building envelopes.

Driving rain is especially important for humidity processes, which are e.g. simulated by WUFI. For this tool a special output format TRY/WUFI can be saved (without driving rain, but with precipitation and wind speed).

Straube's method (Straube, 2001) for calculating the amount of wind driven rain impinging on a wall was selected for use. It was chosen because it is one of the most conservative of the methods generally available and was also the method selected for incorporation into current models (Cornick et al., 2002). It is based on Lacy's method (Lacy, 1965).

The top corner of the building was assumed to be the location of interest; this was used in determining the RAF factor.

$$WDR = RAF \cdot DRF(RR_h) \cdot \cos\theta \cdot FF \cdot RR_h \quad (7.2.44)$$

where: WDR is the wind driven load (mm/h),

RAF is the rain admittance factor. set to 0.9 here,
 RR_h is the horizontal rainfall intensity (mm),
 FF is the wind speed at 10 m above ground (m/s),
and θ is the angle of the wind to the wall normal.

In *METEONORM* WDR is given without the factor $\cos \theta$, if elevation is set to 0.

The driving rain factor DRF can be calculated from:

$$DRF = \frac{1}{V_t} \quad (7.2.45)$$

where: DRF is the driving rain factor
 V_t is the terminal velocity of raindrops (m/s)

The terminal velocity can be calculated from:

$$V_t = -0.16603 + 4.91884 \cdot \Phi - 0.888016 \cdot \Phi^2 + 0.054888 \cdot \Phi^3, \quad \Phi \leq 9.2 \quad (7.2.46)$$

While Straube recommended using D_{50} for the raindrop diameter, the predominant raindrop diameter, D_{pred} , is used here for Φ (like for other current models like MEWS). This is the diameter of drops that accounts for the greatest volume of water in the air.

$$\Phi = D_{pred} = a \cdot \left(\frac{n-1}{n} \right)^{\frac{1}{n}} \approx RR_h^{0.232} \quad (7.2.47)$$

where:

$$a = 1.3 \cdot RR_h^{0.232} \quad (7.2.48)$$

$n = 2.25$

7.2.10 Spectral radiation

For spectral radiation we use the model developed by UMIST in the framework of the EU IST project SoDa. Spectral radiation is used here as an umbrella term for UV bands UVA, UVB and the erythemal radiation (Page and Kift, 2003).

Four UV products are delivered:

- the estimation of UVA radiation between 320 and 400 nm.
- the estimation of UV B irradiation between 290 and 320 nm.
- the estimation of biologically weighted UV radiation, UV erythemal radiation.
- UV Index: clear sky erythemal UV radiation in Wh/m^2 multiplied by a factor 40. This gives a hint on the amount of sun protection needed at clear sky conditions.

A detailed description of the model would exceed the range of this handbook. The model has not yet been validated.

The model consists of 4 main steps:

1. Calculation of the clear sky radiation.
2. Calculation of the overcast radiation.
3. Calculation of mixed situations.
4. Calculation of inclined planes. For this a slightly adopted Perez model is used (chapter 6.7.2).

At each step global and diffuse radiation is calculated. The models were adapted to SMARTS 2 (Gueymard, 1995) output. Linke turbidity, Angström Beta and water vapour are the most important inputs.

7.3 Summary of results

Tables 7.3.1 and 7.3.2 provide a short summary of the main data used in validating the various models and the combined model in Chap. 7.

Tab. 7.3.1: Summary of principal data for interpolation validation.

Model	rmse	
	Monthly means/sums	Yearly means/sums
Interpolation of G_h	24 W/m ² / 15%	22 W/m ² / 13 %
Interpolation of T_a	1.3 °C	1.1 °C
Interpolation of T_d	1.9 °C	1.7 °C
Interpolation of FF	1.2 m/s	1.2 m/s
Interpolation of RR	41 mm	30 mm
Interpolation of R_d	2.4 days	3.5 days
Interpolation of S_d	25.3 hours / 13 %	21.2 hours / 11 %
Interpolation of DD	106 °	74°

Tab. 7.3.2: Summary of principal data for generation model validation.

Model	Resolution	Remarks	mbe	rmse
Generation of N	hour		-0.1 octas	1.8 octas
Calculation of D_h :				
- Hourly model	hour	G_h measured, (rmse: $G_h > 0$)	4 W/m ²	39 W/m ²
- Hourly model	month	G_h generated	4 W/m ²	11 W/m ²
Calculation of G_k :				
- plane inclination 35°	hour	G_h measured, (rmse: $G_h > 0$)	5 W/m ²	33 W/m ²
- plane inclination 90°	hour	G_h measured, (rmse: $G_h > 0$)	3 W/m ²	51 W/m ²
- plane inclination 35°	month	G_h measured	3 W/m ²	5 W/m ²
- plane inclination 90°	month	G_h measured	3 W/m ²	8 W/m ²
- plane inclination 35	month	G_h generated	0 W/m ²	5 W/m ²
- plane inclination 90°	month	G_h generated	7 W/m ²	7 W/m ²

8 Literature

- Aguiar, R. and M. Collares-Pereira (1988): A simple procedure for generating sequences of daily radiation values using a library of markov transition matrices. *Solar Energy*, Vol. 40, No.3, pp. 269-279.
- Aguiar, R. and M. Collares-Pereira (1992): TAG: A time-dependent auto-regressive, Gaussian model. *Solar Energy*, Vol. 49, No.3, pp. 167-174.
- Aubinet, M. (1994): Longwave sky radiation parametrizations. *Solar Energy*, Vol. 53, No.2, pp. 174-154.
- Box, G. O., G.M. Jenkins and G.C. Reinsel. (1994): Time series analysis: Forecasting and control. 3rd edition. Prentice Hall, Englewood Cliffs, NJ.
- Brühwiler, D. (1990): private communication of 7th Nov. concerning calculation of albedo in the DO10 program
- Collier L.R. and J.G. Lockwood (1974): The estimation of solar radiation under cloudless skies with atmospheric dust. *Quart. J. Roy. Meteor. Soc.*, pp. 678-681
- Commission of the European Communities, Directorate General XII for Science, Research and Development (CEC) (1985): Test Reference Year TRY. Weather Data Sets for Computer Simulations of Solar Energy Systems and Energy Consumption in Buildings. 1985 ECSC, EEC, EAEC Brussels and Luxemburg.
- Cornick, S.; Dalglish, A.; Said, N.; Djebbar, R., Tariku, F.; Kumaran, M.K. (2002): Report from Task 4 of MEWS Project. Environmental Conditions Final Report. Institute for Research in Construction National Research Council Canada, Ottawa, Canada K1A 0R6
- Deutscher Wetterdienst (DWD) (1979): Aspirations- und Psychrometertafeln. 6th edition. Friedrich Vieweg&Sohn. Braunschweig/Wiesbaden.
- Dognaux, P. (1975): Variations géographiques et climatiques des expositions énergétiques solaires sur des surfaces réceptrices horizontales et verticales. IRM, Miscsell. B38.
- Dumortier, D. (2002): Prediction of air temperatures from solar radiation. SoDa Deliverable D-5-2-4. Internal document.
- Eidg. Materialprüfungs Anstalt (EMPA) (1985): Proposal for calculating the thermal irradiance of the environment. Draft.
- Gabathuler and Marti (2000): Parametrization of longwave atmospheric radiation at high mountain environments. Draft.
- Gansler, R.A., S.A. Klein and W.A. Beckman (1994): Assessment of the accuracy of generated meteorological data for use in solar energy simulation studies. *Solar Energy*, Vol. 53, No.3, pp. 279 - 287.
- Gilgen H., M. Wild M., A. Ohmura (1998): *Means and trends of shortwave incoming radiation at the surface estimated from Global Energy Balance Archive data.* *Journal of Climate*, 11, 2042-2061.
- Graham, V. and K. Hollands (1990): A method to generate synthetic hourly solar radiation globally. *Solar Energy*, Vol. 44, No.6, pp. 333-341.
- Gueymard C (1995) SMARTS2, a simple model of atmospheric radiative transfer of sunshine: algorithms and performance assessment. Document FSEC-PF-270-95 Florida Solar Energy Centre, 1679 Clearlake Road, Cocoa, Florida, 32922-7703.
- Houghton, J.T., J. Jenkins and J.J. Ephraums (eds.) (1990): Climate Change. The IPCC scientific assessment. Cambridge University Press, Cambridge.
- Iribarne ,J.V. and W.L. Godson (1981): Atmospheric Thermodynamics. D. Reidel Publishing Company, p. 259.

- Kasten, F. (1980): A Simple Parametrization of the Pyrheliometric Formula for Determining the Linke Turbidity Factor. *Meteorol. Rdsch.* 33. 124-127.
- Kasten, F., K. Dehne, H.D. Behr and U. Bergholter (1984): Die räumliche Verteilung der diffusen und direkten Sonnenstrahlung in der Bundesrepublik Deutschland. Federal Ministry of Research and Technology, Research Report No. T 84-125, June 1984.
- Kasten, F. (1990): Höhenabhängigkeit der Globalstrahlung bei wolkenlosem Himmel. Private communication from F. Kasten, DWD, to A. Zelenka, SMA.
- Krist, T. (1976): Formeln and Tabellen der Internationalen Einheiten mit SI-Einheiten. Technik-Tabellen-Verlag Fikentscher & Co., Darmstadt.
- Kunz, S. and R. Volz (1984): Sonnenenergie Nutzungszonen Schweiz (SONUS). Swiss Federal Office of Energy (SFOE), Bern.
- Lacy, R. E. (1965): Driving-Rain Maps and the Onslaught of Rain on Buildings, Proceedings of the RILEM/CIB Symposium on Moisture Problems in Buildings, Helsinki Finland, 1965.
- Lefèvre, M., M. Albuissou and L. Wald (2002): Joint Report on Interpolation Scheme "Meteosat" and Database "Climatology I (Meteosat). SoDa Deliverable D3-8 and D5-1-4. Internal document.
- Lumb, F.E. (1964): The influence of cloud on hourly amounts of total solar radiation at the sea surface. *Quart. J. Roy. Meteor. Soc.* 90, pp. 43-56.
- Müller, G. and A. Ohmura (1993): Radiation Annual Report ETH No.2 1990 and 1991. Zürcher Geographische Schriften (ZGS), No. 52. vdf, Zürich. pp. 17-18.
- Müller, M.J., K. Baltes, E. Lutz, G. Richter and D. Werle (1985): Handbook of Selected World Weather Stations. Soil Erosion Research Group of the University of Trier, Mertensdorf (Ruwertal). 3rd edition.
- Müller-Westermeier, G. (1990): Klimadaten der Bundesrepublik Deutschland, Zeitraum 1951-80. Published by the Deutscher Wetterdienst. Offenbach am Main, 1990.
- Molineaux, B, P. Ineichen and Delauney, J.J. (1995): Direct luminous efficacy and atmospheric turbidity – improving model performance. *Solar Energy* Vol. 55, No. 2, pp. 125-137, 1995.
- NCDC (1995): International Station Meteorological Climate Summary (ISMCS), Version 3.0, March 1995. Fleet Numerical Meteorology and Oceanography Detachment, National Climatic Data Center and USAFETAC OL-A.
- NCDC (2002): Globalsod. Global surface daily data: temperature, precipitation, winds, pressure, snow, etc. (<http://ncdc.noaa.gov>).
- Page, J. K. (1961): The estimation of monthly mean values of daily total short wave radiation on vertical and inclined surfaces from sunshine records for latitudes 40 ° N-40 ° S. Proc. U.N. Conf. on New Sources of Energy, paper No.S 98, 4, 378, (1961).
- Page, J., and R. Kift (2003): Advanced Parameters – Spectral Model. SoDA Deliverable D5-2-5 Internal document.
- Perez, R., R. Stewart, C. Arbogast, R. Seals and J. Scott (1986): An anisotropic hourly diffuse radiation model for sloping surfaces: Description, performance validation, site dependency evaluation. *Solar Energy*, 36, 6, 481-497.
- Perez, R., R. Seals, P. Ineichen, R. Stewart and D. Menicucci (1987): A new simplified version of the Perez Diffuse Irradiance Model for tilted surfaces. *Solar Energy*, Vol. 39, No.3, pp. 221-231.
- Perez, R., P. Ineichen, R. Seals, J. Michalsky and R. Stewart (1990): Modeling daylight availability and irradiance components from direct and global irradiance. *Solar Energy*, Vol. 44, No.5, pp. 271-289.
- Perez, R., P. Ineichen, E. Maxwell, R. Seals and A. Zelenka (1991): Dynamic Models for hourly global-to-direct irradiance conversion. Edited in: Solar World Congress 1991. Volume 1, Part II. Proceedings of the Biennial Congress of the International Solar Energy Society, Denver, Colorado, USA, 19-23 August 1991.
- Perraudeau, M. (1986) : Climat lumineux à Nantes, résultats de 15 mois de mesures. CSTB EN-ECL 86.14L. (1986).

- Remund, J. and S. Kunz (1995): METEONORM – a comprehensive meteorological database and planning tool for system design. In Proceedings of 13th Solar Energy Photovoltaic Conference and Exhibition, Nice. Commission of the European Communities (CEC). Volume I.
- Remund, J. and S. Kunz (1997): Worldwide interpolation of meteorological data. In Proceedings of 14th Solar Energy Photovoltaic Conference and Exhibition, Volume 1, 1997.
- Remund, J., E. Salvisberg and S. Kunz (1998): *Generation of hourly shortwave radiation data on tilted surfaces at any desired location. Solar Energy*. Vol. 62, Nr. 5.
- Remund, J. M. Lefevre, T. Ranchin, L. Wald (2002): Constructing maps of the Linke Turbidity Factor. SoDa Deliverable D5-2-1. Internal document.
- Remund, J. and J. Page (2002): Chain of algorithms: short- and longwave radiation with associated temperature prediction resources. SoDa Deliverable D5-2-2/3. Internal document.
- Richardson, C.W. and D.A. Wright (1984): *WGEN: A model for generating daily weather variables*. U.S. Dept. Agric., Agric. Res. Svc. Pub. No. ARS-8, 83 pp.
- Risoe National Laboratory (1990): *Europäischer Windatlas*. Risoe National Laboratory Roskilde, Dänemark.
- Robinson, N. (ed.) (1966): *Solar Radiation*. Elsevier Publishing Company, Amsterdam, London and New York, 1966.
- sia (1982): sia Recommendation No. 381/3: Heating Degree Days in Switzerland (Heizgradtage der Schweiz). 1982 edition. Swiss Association of Engineers and Architects, PO Box, 8039 Zürich.
- sia (1991): sia Recommendation No. 381/2: Klimadaten zu Empfehlung 380/1 "Energie in Hochbau". 1991 edition. Swiss Association of Engineers and Architects, PO Box, 8039 Zürich.
- sia (1993): sia Recommendation No. 380/1: Energie im Hochbau. 1993 edition. Swiss Association of Engineers and Architects, PO Box, 8039 Zürich.
- Scartezzini, J.-L., M. Nygard Ferguson and F. Bochud (1990): Compression of multi-year meteorological data. Final Report. OFEN Project EF-REN (90)009. Solar Energy and Building Physics Laboratory, Department of Architecture, Swiss Federal Institute of Technology, Lausanne.
- Selker, J.S. and Haither, D.A. (1990): Development and Testing of Single-Parameter Precipitation Distributions. *Water Resources Research* 26(11):2733-2740.
- Sfeir, A.A. and G. Guarracino (1981): *Ingénierie des systèmes solaires TEC&DOC*.
- Skartveit, A., H. Lund. and J.A. Olseth (1992): The Design Reference Year. Recent Advancements in Solar Radiation Resource Assessment. Seminar, Denver, Colorado, November 16-19,1992.
- Straube, J. (2001): Driving Rain Measurement Contract - Final Report, MEWS, Institute for Research in Construction, National Research Council Canada, Ottawa, Canada K1A 0R6
- Swiss Federal Office of Energy (SFOE) (1985): **METEONORM'85**. Infoenergie, Postfach 311, 5200 Brugg, Switzerland.
- Swiss Federal Office of Energy (SFOE) (publ.) (1995): **METEONORM** 1995 edition. Technical Documentation.
- Troll, C. and K. Paffen (1980): *Jahreszeitenklimat der Erde*. (Reduced scale reproduction of wall chart 1:16000000), Berlin 1969.
- Unsworth, M.H. et al. (1975): Longwave radiation at the ground. *Quarterly Journal of the Royal Meteorological Society*.
- Vose, R.S., R.L. Schmoyer, P.M. Steurer, T.C. Peterson, R. Heim, T.R. Karl and J.K. Eischeid (1992): The Global Historical Climatology Network: long-Term Monthly Temperature, Precipitation, Sea Level Pressure and Station Pressure Data (NDP-041). Downloadable from Carbon dioxide information analysis center (<http://cdiac.ornl.gov>).
- Wald, L. and M. Lefèvre (2001): Interpolation schemes - Profile Method (a process-based distance for interpolation schemes). SoDa Deliverable D5-1-1. Internal document.
- World Meteorological Organisation (WMO) (1971): Climatological Normals (Clino) for climate and climate ship stations for the period 1931-60. WMO/OMM - No.117.TP.52.

- World Meteorological Organisation (WMO) (1998): 1961 – 90 Climatological Normals (Clino). Version 1.0 – November 1998. CD-ROM.
- Wright, J., R. Perez and J.J. Michalsky (1989): Luminous Efficacy of Direct Irradiance: Variation with Moisture Conditions. *Solar Energy*, Vol. 42, pp. 387-394.
- Zentralanstalt für Meteorologie und Geodynamik (ZAMG) (1994): Wetter- und Klimaübersicht Januar - Dezember 1994.
- Zelenka, A., G. Czeplak, V. D'Agostino, J. Weine., E. Maxwell., R. Perez, M. Noia, C. Ratto and R. Festa (1992): Techniques for supplementing solar radiation network data, Volume 1-3. IEA Report No. IEA-SHCP-9D-1.